International Journal of Engineering

Journal Homepage: www.ije.ir

Application of a Novel Optimization Algorithm in Design of Lead Rubber Bearing Isolation Systems for Seismic Rehabilitation of Building Structures

F. Mehri[a], S. Mollaei*[a], E. Noroozinejad Farsangi*[b], M. Babaei[a], F. Ghahramani[c]

[a] *Department of Civil Engineering, University of Bonab, Bonab, East Azerbaijan, Iran*
[b] *Faculty of Civil and Surveying Engineering, Graduate University of Advanced Technology, Kerman, Iran*
[c] *Department of Civil Engineering, Urmia University, Urmia, Iran*

PAPER INFO

Paper history:
Received 03 January 2023
Received in revised form 26 January 2023
Accepted 28 January 2023

Keywords:
Lead Rubber Bearing Isolator
Optimization
Mass Irregularity
Near-Fault Earthquake

ABSTRACT

Various mechanical and geometrical parameters have different effects on the isolation system's performance. Thus, a sensitivity study of the isolated structures' behavior is an essential matter. In this regard, the isolation systems should be designed using optimization approaches to consider the effects of the different factors. In this study, the optimal design of the lead rubber bearing (LRB) seismic isolation was conducted by considering mass irregularity and near-fault seismic excitation effects. Also, sensitivity analysis of the behavior of the considered isolated buildings was implemented concerning the mechanical parameters of the LRB system. A nonlinear time history dynamic analysis was used here, and the design optimization of the LRB isolator was programmed using the newly introduced grasshopper optimization algorithm (GOA). The main purpose was to investigate the ability of the GOA to optimize the design parameters of the LRB-isolated frames. The results proved the desirable ability of the GOA to solve optimal design problems for isolation systems. Also, the sensitivity analysis of the seismic behavior of LRB base-isolated structures showed that the yield base shear index had the most important effects. Also, the mass irregularity parameter showed a negligible influence.

***doi**: 10.5829/ije.2023.36.03c.20*

1. INTRODUCTION

During ground motions, structures vibrate, and if the structures have weak energy dissipation, they will be damaged, and in more severe cases, the structures will be collapsed. In recent decades, extensive studies have been conducted on developing structural control systems for the robust design of structures under seismic excitations [1-5]. In structural control systems, the mechanism of control devices has a significant role in the energy dissipation caused by earthquakes. A seismic isolation system with suitable force-displacement hysteresis properties can have the desired characteristics, such as optimum flexibility, high damping, and reduction of horizontal earthquake forces [6]. The primary purpose of the seismic isolation method is to prevent the transfer of horizontal ground motions and seismic forces to the superstructure. The reduction of transmitted seismic force to the superstructure is achieved by increasing the natural period of the structure and energy dissipation at the isolation level [7]. One of the most common types of isolation systems is the lead rubber bearing (LRB).

The seismic behavior of isolated structures is affected by different parameters. Various studies have been conducted to evaluate the behavior of the isolation system. In some studies, the impact of the type and mechanical parameters of the isolator has been assessed [8, 9]. Also, the effect of soil interaction on the isolation system [10, 11], isolation in tall buildings [12], evaluation of fragility curves in system isolation [13], reliability analysis [14], and reliability-based design [15] in isolated systems, semi-active isolation systems [16], hybrid control strategies for the isolated structures [17, 18], optimization of the shape memory alloy based friction pendulum system [19], and the cost benefits of isolations in the seismic design of structures [20] have

*Corresponding Authors Institutional Emails: s.mollaei@ubonab.ac.ir (S. Mollaei) & noroozinejad@kgut.ac.ir (E. Noroozinejad)

Please cite this article as: F. Mehri, S. Mollaei, E. Noroozinejad Farsangi, M. Babaei, F. Ghahramani, Application of a Novel Optimization Algorithm in Design of Lead Rubber Bearing Isolation Systems for Seismic Rehabilitation of Building Structures, ***International Journal of Engineering, Transactions C: Aspects,*** Vol. 36, No. 03, (2023) 594-603

been studied. Shaking table experiments have been carried out on base-isolated building systems [21]. Recently, the Telescopic Column (TC) system was proposed as a novel rocking-isolation method by Farsangi et al. [22].

Also, some studies showed that the performance of the isolation systems can be affected by factors such as geometric conditions, the irregularity of the structure, and seismic excitation characteristics. The damage caused by earthquakes depends on many factors, such as failure mechanism, site location, soil type, and earthquake record characteristics, including frequency content, duration, and amplitude [23]. Some researchers have studied the effects of ground motion [24], the impact of horizontal and vertical components [25], and the effect of earthquake frequency content [26] on the performance of isolated systems. The effects of near-fault and far-fault earthquakes have also been considered in some other studies [27-29]. In several studies, the effects of asymmetry in structure [30], the presence of soft stories [31], and eccentricity [32] on isolated structures have been studied. An isolated building with LRB isolators was analyzed using a series of real near-fault earthquake ground accelerations [33].

Determining the mechanical parameters of isolator devices to achieve efficient performance for the isolation system is a complex process. However, studies have shown that the behavior of these systems can be influenced by various conditions. Therefore, the design of isolation systems is defined in the framework of design optimization problems. One of the efficient methods in solving engineering optimization problems is meta-heuristic algorithms [34, 35]. So far, several metaheuristic algorithms have been introduced, such as charged system search (CSS), colliding bodies optimization (CBO), vibrating particle system (VPS) [34], ant colony optimization (ACO) [36], grasshopper optimization algorithm (GOA) [37], and so on. Recently, the particle swarm optimization algorithm was used to optimize the magneto-rheological (MR) damper parameters [38].

The literature review proved that more investigation is necessary for the optimization of the base isolation design process, especially when using novel optimization algorithms. In this study, the optimum design of a seismic isolation system with LRB isolators is solved using the newly introduced method of GOA while considering the mass irregularity and near-fault earthquake effects. The main purpose here is to evaluate the GOA method for optimizing the design of the LRB-isolated system.

2. MATERIALS AND METHODS

2. 1. Seismic Isolation Systems Rubber supports can provide the flexibility and deformation required for vibration isolation. If these supports are combined with a lead core to dissipate input energy, the necessary damping is also offered for the system. The shear deformation of the lead core in rubber supports can be controlled by using steel plates in the system. So, the lead core deforms against shear forces and causes a bilinear hysteresis behavior in the device [39]. Also, the rubber part of this isolation system is responsible for providing the restoration force (Figure 1 (a)).

In practice, all LRB isolation systems are simulated with a bilinear hysteresis model based on the three parameters of elastic stiffness (K_1), post-yield stiffness (K_2), and specified yield strength (Q_y), as shown in Figure 1 (b). The post-yield stiffness is obtained from the desired period of the structural system. For lead rubber bearing (LRB) and frictional pendulum systems (FPS), elastic stiffness is a coefficient of post-yield stiffness [28].

Initially, a time period is selected for the isolated structure (T_2) at the design displacement level, usually between 2 and 3 seconds. Then the post-yield stiffness of the isolated system for the selected period can be calculated using Equation (1):

$$K_2 = M \times \left(\frac{2\pi}{T_2}\right)^2 \quad (1)$$

In this relationship, M is the total mass of the whole structure isolated at the base. Also, the yield shear strength at the isolation level (Q_y) can be defined using Equation (2):

$$Q_y = \alpha M g \quad (2)$$

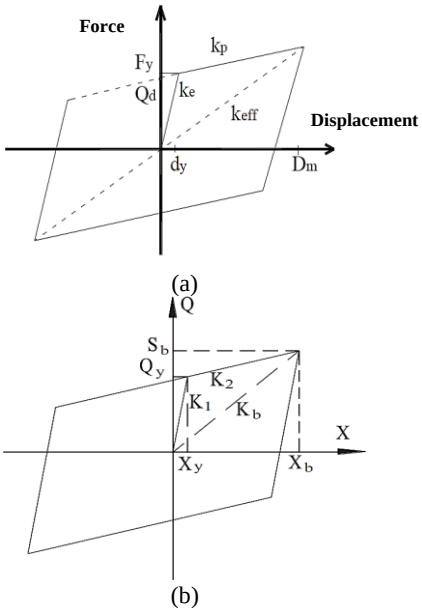

Figure 1. (a) Hysteretic loops parameters [40]; and (b) A bilinear behavioral model the LRB isolation used in this study [28]

In this relationship, α is the yield shear coefficient. Assuming a value between 0 and 1, the effective shear force on the structure can be determined. In the bilinear behavioral model, the value of the elastic stiffness of the system (K_1) can be determined by selecting the yield deformation component (X_y) as the elastic behavior limit.

$$K_1 = \frac{Q_y}{X_y} \tag{3}$$

Therefore, the ratio of initial stiffness to post-yield stiffness is defined as the parameter α_k in relation (4):

$$\alpha_k = \frac{K_1}{K_2} \tag{4}$$

Also, the damping of the isolation system (c_b) in terms of the effective damping ratio (ξ_b), which represents the dissipated energy, is equal to Equation (5):

$$c_b = 2\xi_b\sqrt{K_2 \times M} \tag{5}$$

2. 2. Nonlinear Dynamic Analysis The dynamic response of a structural system beyond its linear elastic range can usually not be calculated by an analytical solution. Even if the excitation changes are described by a simple function. Therefore, using numerical methods in the analysis of nonlinear systems is necessary. The Newmark method with a modified Newton-Raphson iteration approach is generally used for nonlinear dynamic equation solutions [41].

The dynamic equation of a structure with nonlinear behavior is written as Equation (6):

$$M\ddot{U}(t) + C\dot{U}(t) + F_S(t) = P(t) \tag{6}$$

where t is the time; U, $\dot{U}$ and $\ddot{U}$, are displacements, velocities, and acceleration vectors relative to the ground, respectively; M is the mass matrix; C is the damping matrix; F_S is the vector of resisting forces, which is a function of displacement and P(t) is the applied force, which for the seismic case is given by ground acceleration time history. Also, the initial condition is $U(0) = U_0$ and $\dot{U}(0) = \dot{U}_0$. According to the equilibrium conditions in each time interval, the equation of motion during the time step t_{i+1} can be written as follows:

$$M\ddot{U}_{i+1} + C\dot{U}_{i+1} + F_{s_{i+1}} = P_{i+1} \tag{7}$$

In this paper, the constant average acceleration method with Newton–Raphson iterations has been used to analyze the nonlinear MDOF structures. At first, the initial state of the structural system is determined (K_{T0} and F_{s0}). Then, also, the initial acceleration is calculated:

$$\ddot{U}_0 = M^{-1}\left(P_0 - C\dot{U}_0 - F_{s0}\right) \tag{8}$$

then for each time step:

$$\bar{P}_{i+1} = P_{i+1} + a_1U_i + a_2\dot{U}_i + a_3\ddot{U}_i \quad , \quad i = 0.1.2.\ldots \tag{9}$$

where:

$$a_1 = \left(\frac{1}{\beta(\Delta t)^2}\right)M + \left(\frac{\gamma}{\beta\Delta t}\right)C \tag{10}$$

$$a_2 = \left(\frac{1}{\beta\Delta t}\right)M + \left(\frac{\gamma}{\beta} - 1\right)C \tag{11}$$

$$a_3 = \left(\frac{1}{2\beta} - 1\right)M + \Delta t\left(\frac{\gamma}{2\beta} - 1\right)C \tag{12}$$

If the resisting forces are not equal to the applied force, a residual force vector is defined as:

$$\bar{R}_{i+1} = \bar{P}_{i+1} - (F_s)_{i+1} - a_1U_{i+1} \tag{13}$$

By using the Newton–Raphson iteration method, the additional displacement due to this residual force is determined by solving:

$$\Delta U = (\bar{K}_T)_{i+1}{}^{-1} \times \bar{R}_{i+1} \tag{14}$$

where $\bar{K}_T$ is the tangent stiffness that can be considered as follows:

$$(\bar{K}_T)_{i+1} = (K_T)_{i+1} + a_1 \tag{15}$$

The responses of a nonlinear structure can be obtained as follows:

$$U_{i+1} = U_i + \Delta U \tag{16}$$

$$\dot{U}_{i+1} = \left(\frac{\gamma}{\beta\Delta t}\right)\Delta U + \left(1 - \frac{\gamma}{\beta}\right)\dot{U}_i - \Delta t\left(1 - \frac{\gamma}{2\beta}\right)\ddot{U}_i \tag{17}$$

$$\ddot{U}_{i+1} = \left(\frac{1}{\beta(\Delta t)^2}\right)\Delta U - \left(\frac{1}{\beta\Delta t}\right)\dot{U}_i + \left(1 - \frac{1}{2\beta}\right)\ddot{U}_i \tag{18}$$

where γ and δ are Newmark parameters, in this study, $\gamma = 0.5$ and $\delta = 0.25$ have been used for nonlinear analysis of the structure.

2. 3. Grasshopper Optimization Algorithm Optimization methods in their classical form use the derivation information of the objective function to find the optimal solution. These methods fall into the locale optimum points for complex problems, and cannot be used for underivable functions. Another type of optimization methods are stochastic methods, such as meta-heuristic algorithms. These methods are generally population-based algorithms inspired by nature. One of the evolutionary algorithms is the grasshopper optimization algorithm (GOA) which is inspired by the grasshopper lifecycle [37]. Most of the nature-inspired algorithms divide the search area into exploration and exploitation parts. In the exploration step, search agents are driven by random movements, while, in the exploitation phase, they tend to move locally around their place.

The theoretical model used to simulate grasshoppers' behavior was initially in the form of Equation (19):

$$X_i = S_i + G_i + A_i \tag{19}$$

where X_i indicates the position of the grasshopper *i*, S_i is the social interaction, G_i is the force of gravity applied to the grasshopper *i*, and A_i represents the direction of the wind. The value of S_i, that is, the social interaction for grasshopper *i*, is calculated by Equation (20):

$$S_i = \sum_{j=1}^{N} S(d_{ij})\widehat{d_{ij}} \quad (20)$$

where d_{ij} indicates the distance between grasshoppers *i* and *j* and is calculated as Equation (21):

$$d_{ij} = |x_i - x_j| \quad (21)$$

as shown in Equation (20), $\widehat{d_{ij}}$ is a unit vector from the *i*th to the *j*th grasshopper. *S* is also a function for defining social force. The function *S*, which defines a social force, is calculated as in Equation (22):

$$S(r) = fe^{\frac{-r}{l}} - e^{-r} \quad (22)$$

where f represents the intensity of gravity, and I represents the length of the gravity scale. Parameters I and f significantly change the comfort zone, attraction, and repulsion.

Research has shown that the initial grasshopper motion relationship cannot be used in swarm simulation and optimization algorithms since this relationship prevents exploration and exploitation in the search space around a solution. The model is used for outdoor crowding. Therefore, Equation (23) has been used and can simulate the interaction between the grasshoppers in the swarm.

$$x_i^d = c\left(\sum_{j=1}^{N} c\frac{ub_d - lb_d}{2} s(|x_j^d - x_i^d|)\frac{x_j - x_i}{d_{ij}}\right) + \widehat{T_d} \quad (23)$$

Where ub_d is the upper bound in the *d*-th dimension, and lb_d is the lower bound in the *d*-th dimension. $\widehat{T_d}$ is the value of the *d*-th dimension in the target (the best solution ever seen), and *c* is a decreasing constant to reduce the area of comfort, repulsion, and attraction.

In Equation (23), *S* is obtained from Equation (19), and the parameters of gravity (*G*) and wind direction (*A*) are not considered. Based on this equation, the next position of a grasshopper can be defined using its current position, the target position, and the positions of all other grasshoppers. To maintain a balance between exploration and exploitation, parameter *c* needs to decrease with increasing repetition times during the algorithm. The coefficient *c* reduces the comfort zone in proportion to the number of repetitions (Equation (24)):

$$c = c_{max} - i\frac{C_{max} - C_{min}}{l} \quad (24)$$

where C_{max} is the maximum value, C_{min} is the minimum value, i represents the current iteration number, and l is the maximum number of algorithm iterations. In the simulations, the value of C_{max} is 1 and the value of C_{min} is 0.00001.

2. 4. Design Formulation Design variables are a set of parameters that affect design details and design results. Different parameters affect the design of base isolation systems in building structures. Parameters that are independently involved in the behavior mechanism of Lead Rubber Bearings are selected as design variables. The behavioral model of any Lead Rubber Bearing is influenced by independent factors such as yield displacement (X_y), secondary time period (T_2), base shear yield coefficient (α), damping ratio (ξ_b), etc., that parameters such as initial hardness (K_1), Secondary stiffness (K_2), yield shear strength (Q_y) and damping coefficient (c_b) are functions of these changes. In the optimum design of a Lead Rubber Bearing, these parameters are selected as the design variables. Constraints on the optimum design of isolations apply to the design variables due to physical limitations and acceptable results. According to the above, the optimum design of Lead Rubber Bearing for building structures is formulated as Equation (25):

$$Find: Design\ Variables\ X = \begin{Bmatrix} X_y \\ T_2 \\ \alpha \\ \xi_b \end{Bmatrix}$$

$$which\ minimizes\ Objective\ Function: f(X) \quad (25)$$

$$Subject\ to: \begin{cases} X_{y_{min}} \le X_y \le X_{y_{max}} \\ T_{2_{min}} \le T_2 \le T_{2_{max}} \\ \alpha_{min} \le \alpha \le \alpha_{max} \\ \xi_{b_{min}} \le \xi_b \le \xi_{b_{max}} \end{cases}$$

In this paper, the objective function for the optimization problem is defined based on performance indices for inter-story drift. This index shows the effect of control devices on system performance and is expressed based on the ratio of controlled maximum drift response to uncontrolled maximum response:

$$Objective\ Function = f(\mathrm{X}) = \left|\frac{Max(drift_{i,Controlled})}{Max(drift_{i,Uncontrolled})}\right| \quad (26)$$

where $drift_i$ is the inter-story drift of the *i*-th story.

The iteration process of the proposed algorithm has been summarized in Table 1 for steps i to i + 1. Also, the procedure of finding the displacement, velocity, and acceleration responses for the next steps are summarized in Table 2.

2. 5. Numerical Case Studies In this article, the numerical studies include three cases:

Case 1: In the first case, the seismic behavior of the base-isolated building structure with LRB is analyzed for sensitivity to evaluate the effect of LRB mechanical parameters and the mass irregularity of the structure.

TABLE 1. Summary of the steps of Newton-Raphson method used here

1) Data definition: $u_{i+1}^{(0)} = u_i$, $f_S^{(0)} = (f_S)_i$, $\Delta R^{(1)} = \Delta\hat{p}_i$, $\hat{K}_T = \hat{K}_i$
2) Iterative calculations (j=1,2, …): $\hat{K}_T \Delta u^{(j)} = \Delta R^{(j)} \rightarrow \Delta u^{(j)}$, $u_{i+1}^{(j)} = u_{i+1}^{(j-1)} + \Delta u^{(j)}$ $\Delta f^{(j)} = f_S^{(j)} - f_S^{(j-1)} + (\hat{K}_T - K_T)\Delta u^{(j)}$, $\Delta R^{(j+1)} = \Delta R^{(j)} - \Delta f^{(j)}$
3) Repeating (j→j+1)

TABLE 2. Steps of the Newmark method used here

Average acceleration method $\beta = \frac{1}{4}, \gamma = \frac{1}{2}$
1) Initial calculations: $\ddot{u}_0 = \frac{p_0 - c\dot{u}_0 - (f_s)_0}{m}$
1-2) Determination of the Δt : $a = \frac{1}{\beta \Delta t} m + \frac{\gamma}{\beta} c$, $b = \frac{1}{2\beta} m + \Delta t \left(\frac{\gamma}{2\beta} - 1\right) c$
2) Iterative calculations: $\Delta\hat{p}_i = \Delta p_i + a\dot{u}_i + b\ddot{u}_i$
2-1) Determination of the tangential stiffness (K_i) : $\hat{k} = k + \frac{\gamma}{\beta \Delta t} c + \frac{1}{\beta (\Delta t)^2} m$
2-2) Determination of the Δu using the updated Newton-Raphson method and Table 1: $\Delta\dot{u}_i = \frac{\gamma}{\beta \Delta t}(\Delta u_i) + -\frac{\gamma}{\beta}\dot{u}_i + \Delta t \left(1 - \frac{\gamma}{2\beta}\right)\ddot{u}_i$, $\Delta\ddot{u}_i = \frac{1}{\beta (\Delta t)^2}(\Delta u_i) - \frac{1}{\beta \Delta t}\dot{u}_i - \frac{1}{2\beta}\ddot{u}_i$ $\ddot{u}_{i+1} = \ddot{u}_i + \Delta\ddot{u}_i$, $\dot{u}_{i+1} = \dot{u}_i + \Delta\dot{u}_i$, $u_{i+1} = u_i + \Delta u_i$
3) Repeating (i→i+1)

Case 2: In the second case, the LRB isolation system is designed using the GOA meta-heuristic optimization method. To have a comprehensive comparison of GOA algorithm performance, some of the well-known metaheuristic algorithms, such as Particle Swarm Optimization (PSO), Harmony Search (HS), and Colliding Body Optimization (CBO), are selected to solve the optimum design of LRB.

Case 3: Finally, in the third case, the seismic behavior of isolated building structures with optimized LRB isolators using GOA with the best solution is evaluated under near-fault earthquakes and mass irregularities, and the performance of LRB isolators is compared in different conditions.

For numerical studies, benchmark structural models are used. These structural models include two models of 5-story (Example 1) and 10-story (Example 2) building structures. These structures have a two-dimensional lumped mass shear building system. The mechanical properties of the considered structures, such as mass, stiffness, and damping, are assumed to be the same for all the stories. The mass and stiffness of each story are respectively 445 ton and 448 MN/m for 5-story models; those values are respectively 252.1 ton and 354.2 MN/m in the 10-story models. For these models, the damping ratio (ξ_s) is assumed to be 0.02 and the damping coefficient (c) for each story can be calculated using Riley method. Also, the reference structural models are drawn in Figure 2.

To calculate the seismic responses and optimize the design of the LRB isolator, the generated Gaussian random white noise with a duration of 40 seconds and a maximum acceleration of 0.35 g is used as ground motion acceleration (Figure 3). Also, the ground acceleration of near-fault earthquakes is used to study the seismic behavior of isolated building structures with the optimal LRB system. According to many of the past studies [42-44] and seismic design guidelines, the recordings of three real earthquakes were utilized in this research. The Imperial Valley, the Northridge, and the Chi-Chi earthquakes were used here. The details of the considered earthquakes are presented in Table 3, which are selected from the Pacific earthquake Engineering Research Center (PEER). Irregular conditions for building models are defined based on mass irregularities in the height of the

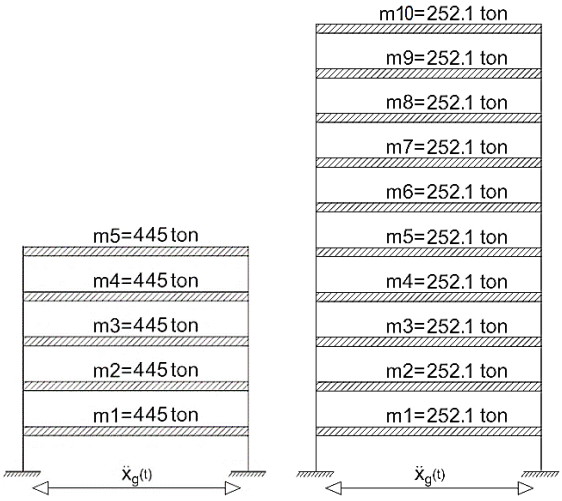

Figure 2. Reference structural models considered here

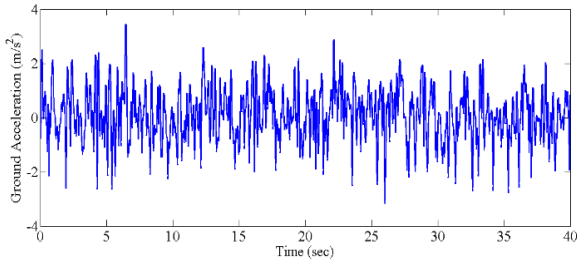

Figure 3. Time history of ground acceleration in random white noise (W(t))

TABLE 3. Details of earthquakes used in this study [28]

Event	Station	Magnitude	Distance (km)	PGA ($\frac{m}{s^2}$)	$\frac{PGV}{PGA}$
Imperial Valley	El Centro	6.5	1.35	4.40	0.26
Northridge	NWH-360	6.7	6.8	5.79	0.17
Chi-Chi	TCU-052	7.6	1.84	3.56	0.52

structure. Irregularity for this building model is defined as a 50% variation in the mass of successive stories.

3. RESULTS AND DISCUSSION

To show the effect of each parameter of the isolator on system performance, the sensitivity analysis is used here. To achieve this aim, the sensitivity of the seismic responses of isolated structures with LRB is evaluated in relation to changes in the values of the yield base shear coefficient, secondary period, yield displacement, damping coefficient, and mass irregularity. Every parameter changes incrementally in the allowable range of parameters. The changes in maximum inter-story drift responses for each component are shown in Figures 4 and 5 for 5 and 10- story building models, respectively. As shown in Figures 4 and 5, the structural drift response has a high sensitivity to the yield base shear ratio. Also, the mass irregularity does not have a considerable effect on the performance of isolated structures.

In the second part, the results obtained from solving the optimization problem in the design of isolation systems with LRB isolators are presented. The outputs of

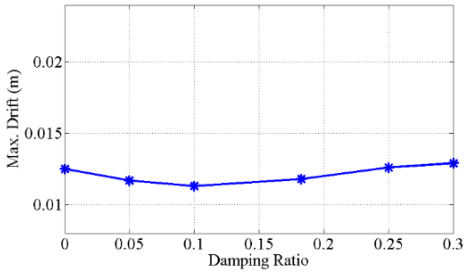

(c)

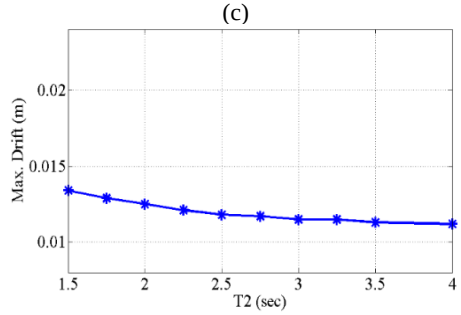

(d)

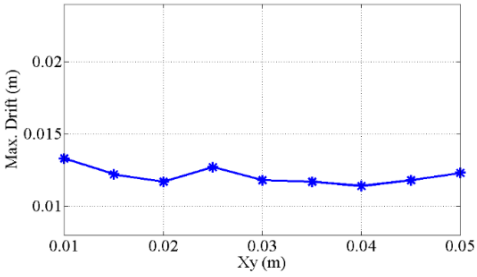

(e)

Figure 4. The variation of maximum drift response in a 5-story isolated building structure relative to: (a) mass irregularity; (b) base shear ratio; (c) Damping; (d) secondary time period; (e) yield displacement

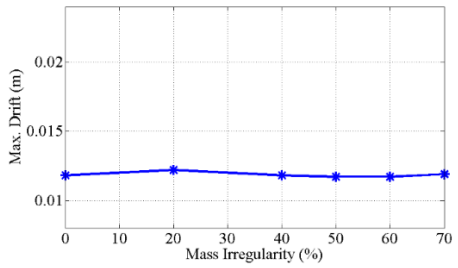

(a)

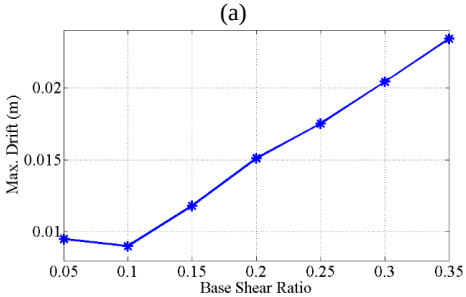

(b)

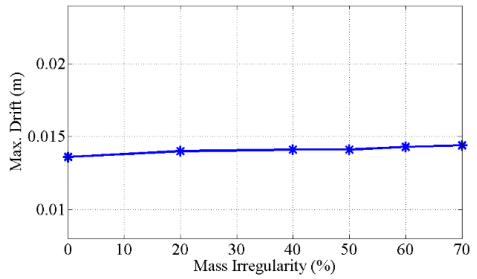

(a)

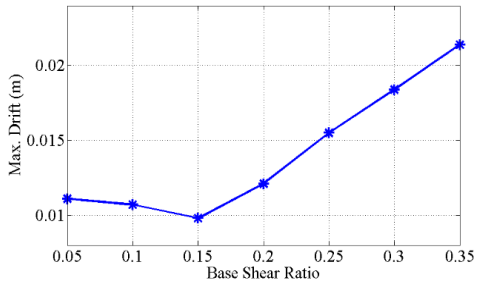

(b)

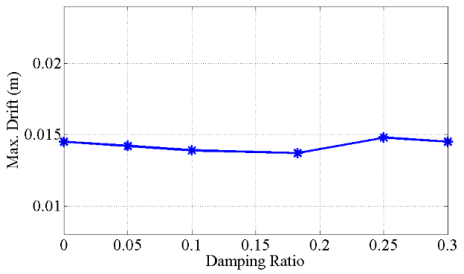

(c)

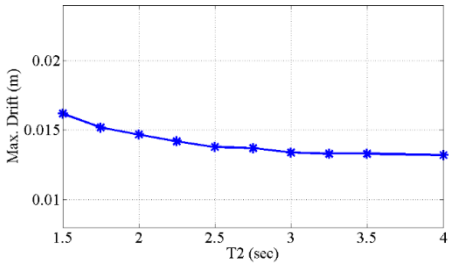

(d)

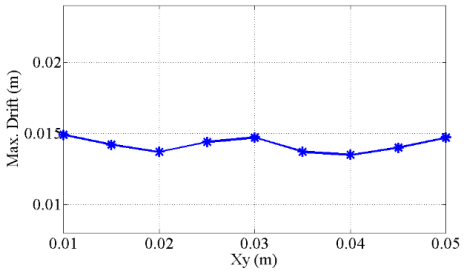

(e)

Figure 5. The variation of maximum drift response in a 10-story isolated building structure relative to: (a) mass irregularity; (b) base shear ratio; (c) Damping; (d) secondary time period; (e) yield displacement

this problem include the convergence history of the objective function, the minimum value calculated for the objective function, and the optimal values of design variables. Figure 6 shows the convergence history diagram for the defined objective function based on controlled seismic responses in the isolated building with LRB isolators for the GOA. According to this method, the minimum value for the ratio of maximum controlled responses to uncontrolled responses for the 5-story structural models is 0.19995, and for 10-story structural models, it is 0.4058.

In order to perform a comprehensive evaluation of the performance of the algorithms, a statistical test was performed based on the best solution, the mean, and the standard deviation of the solutions. The results of statistical tests for the GOA algorithm compared to PSO, HS, and CBO algorithms to solve the optimum design of the base isolation system are presented in Table 4. This statistical test was performed for each 5 and 10-story building structure case study based on 30 independent runs. According to the results of this test, in Table 4, the GOA algorithm shows its stability and robustness for solving the LRB design problem. Table 5 shows the results obtained from the optimal design of LRB isolators using GOA, including design variables and constraints for 5 and 10-story structural models.

Finally, the seismic behavior of isolated building structures using optimized LRB isolators is evaluated in both regular and mass irregularity cases under near-fault earthquakes. In this regard, the time history of seismic inter-story drift response at the maximum level is compared to the near-fault records of the Imperial Valley, Northridge, and Chi-Chi. Figures 7 to 9 show the drift time history of a 5-story structure for each earthquake. Under the Imperial Valley earthquake, the maximum drift is 0.95 cm for the regular 5-story structural model and 0.99 cm for the irregular 5-story structural model. For the Northridge earthquake, the maximum drift is 0.72 cm for the regular 5-story structural model and 0.70 cm for the irregular 5-story structural model. Also, under the Chi-Chi earthquake, the maximum drift value is 1.10 cm for the regular 5-story structural model and 1.05 cm for the irregular 5-story structural model.

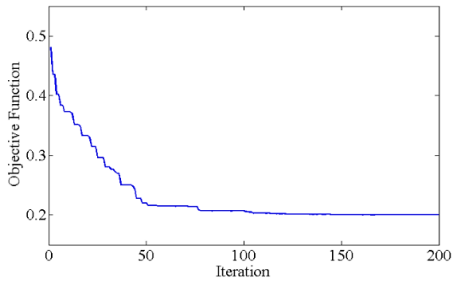

(a)

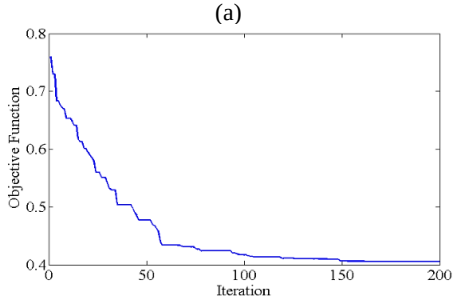

(b)

Figure 6. Convergence history of the objective function for the design of LRB with the GOA (a) 5-story (b) 10-story

TABLE 4. Statistical test for the optimization problem

Model	Test	PSO	HS	CBO	GOA
5-story	Best	0.21754	0.25736	0.24328	0.19995
	Mean	0.25641	0.29768	0.27585	0.22584
	STD	0.04743	0.05303	0.04538	0.02461
10-story	Best	0.41886	0.46629	0.45043	0.40579
	Mean	0.45718	0.50906	0.48452	0.43041
	STD	0.04938	0.05954	0.04489	0.03615

TABLE 5. Optimal design results for the LRB isolator with GOA algorithm

Set	Parameter	Dimension	Value	
			5- Story	10- Story
Objective Function	Controlled Responses	-	0.19995	0.40579
Design Variables	Yield Base Shear Ratio (α)	-	0.055024	0.058653
	Yield Deformation (X_y)	cm	0.019219	0.038141
	Secondary Period (T_2)	s	2.9937	3.9946
	Damping Ratio (ζ_b)	%	0.20751	0.13873
Constraints	Stiffness Ratio (α_k)	-	0.1569	0.16407
	Isolator Deformation	cm	0.20127	0.3849

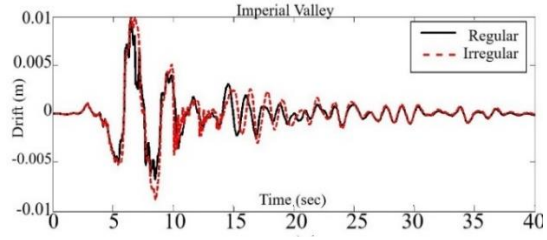

Figure 7. Time history of maximum drift for the 5-story model under Imperial Valley earthquake

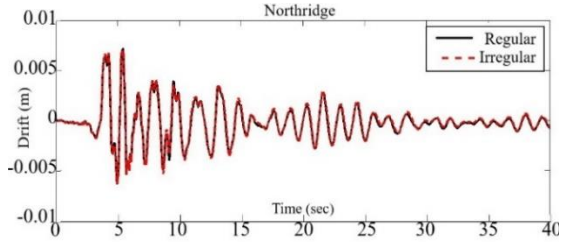

Figure 8. Time history of maximum drift for the 5-story model under Northridge earthquake

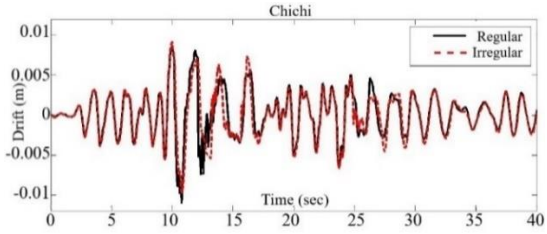

Figure 9. Time history of maximum drift for the 5-story model under the Chi-Chi earthquake

Figures 10 to 12 show the time history of maximum drift for a 10-story structure under each earthquake. Under the Imperial Valley earthquake, the maximum drift is 1.53 cm and 1.60 cm for the regular and irregular 10-story structural models, respectively. For the

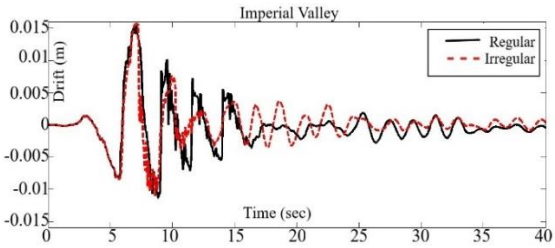

Figure 10. Time history of maximum drift for the 10-story model under Imperial Valley earthquake

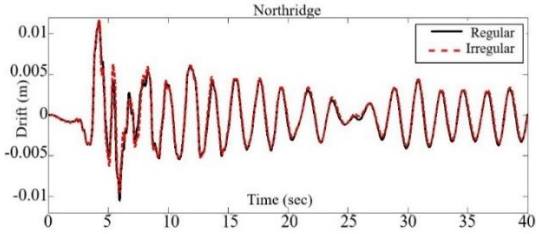

Figure 11. Time history of maximum drift for the10-story model under Northridge earthquake

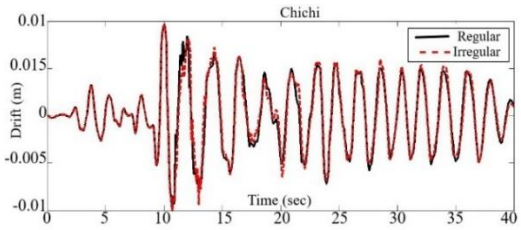

Figure 12. Time history of maximum drift for the 10-story model under the Chi-Chi earthquake

Northridge earthquake, the maximum drift for a 10-story structural model in both regular and irregular modes is 1.16 cm. Also, under the Chi-Chi earthquake, the maximum drift value for a model of 10-story structures in both regular and irregular modes is 1.00 cm. As can be seen, the presence of irregularities in the isolated structure does not affect the drift response of the structure under near-fault earthquakes. The existence of mass irregularity in the structure can lead to a change in the main period time of the structure and, consequently, a change in the seismic behavior of the structure. However, the use of seismic isolators at the base of building structures increases the main period of the structure. And it creates distance from the dominant frequencies of ground motion.

4. CONCLUSIONS

The primary purpose of this study was to optimum design a lead rubber-bearing seismic isolation system and evaluate the effects of mass irregularity and near-fault

seismic excitation on the seismic responses of buildings. Also, the sensitivity analysis of the isolated structures to the mechanical parameters of the lead-rubber bearing system and the mass irregularity was conducted here.

For numerical studies, two models of 5- and 10-story building structures with lumped mass shear frame systems were selected. The seismic behavior of these structures was studied under regularity and irregularity of mass conditions and in two fixed base and isolated cases with the LRB isolator. The LRB system's characteristics were optimally designed using GOA.

The sensitivity analysis of the seismic behavior of the LRB-isolated structures showed that the yield base shear ratio is the most influential parameter. According to the results of statistical tests comparing the GOA algorithm to the PSO, HS, and CBO algorithms to solve the optimum design of the base isolation system, the GOA has an excellent ability to solve the optimization problem of the isolation system design for building structures. The seismic performance of LRB isolation systems, which were optimally designed for regular structures, was not affected by mass irregularities in the structure. Also, the LRB isolation system had the identical performance in controlling the seismic responses of structures in the presence of mass irregularity under near faults earthquakes for both 5- and 10-story models. In other words, the performance of LRB isolators was not degraded by changes in the height of building structures.

5. REFERENCES

1. Spencer Jr, B. and Soong, T., "New applications and development of active, semi-active and hybrid control techniques for seismic and non-seismic vibration in the USA", in Proceedings of international post-SMiRT conference seminar on seismic isolation, passive energy dissipation and active control of vibration of structures, Cheju, Korea., (1999), 23-25.
2. Farsangi, E.N., Takewaki, I., Yang, T.Y., Astaneh-Asl, A. and Gardoni, P., "Resilient structures and infrastructure, Springer, (2019).
3. Pal, S., Roy, B. and Choudhury, S., "Comparative performance study of tuned liquid column ball damper for excessive liquid displacement on response reduction of structure", ***International Journal of Engineering, Transactions B: Applications,*** Vol. 33, No. 5, (2020), 753-759. https://doi.org/10.5829/ije.2020.33.05b.06
4. Barkhordari, M. and Tehranizadeh, M., "Ranking passive seismic control systems by their effectiveness in reducing responses of high-rise buildings with concrete shear walls using multiple-criteria decision making", ***International Journal of Engineering***, ***Transactions B: Applications,*** Vol. 33, No. 8, (2020), 1479-1490. http://dx.doi.org/10.5829/ije.2020.33.08b.06
5. Basu, B., Bursi, O.S., Casciati, F., Casciati, S., Del Grosso, A.E., Domaneschi, M., Faravelli, L., Holnicki-Szulc, J., Irschik, H. and Krommer, M., "A european association for the control of structures joint perspective. Recent studies in civil structural control across europe", ***Structural Control and Health Monitoring***, Vol. 21, No. 12, (2014), 1414-1436. http://dx.doi.org/10.1002/stc.1652
6. Soong, T. and Spencer Jr, B., "Supplemental energy dissipation: State-of-the-art and state-of-the-practice", ***Engineering Structures***, Vol. 24, No. 3, (2002), 243-259. https://doi.org/10.1016/S0141-0296(01)00092-X
7. Cheng, F.Y., "Smart structures: Innovative systems for seismic response control, CRC press, (2008).
8. Matsagar, V.A. and Jangid, R., "Influence of isolator characteristics on the response of base-isolated structures", ***Engineering Structures***, Vol. 26, No. 12, (2004), 1735-1749. http://dx.doi.org/10.1016/j.engstruct.2004.06.011
9. Tamim Tanwer, M., Kazi, T.A. and Desai, M., "A study on different types of base isolation system over fixed based", in Information and Communication Technology for Intelligent Systems: Proceedings of ICTIS 2018, Volume 1, Springer., (2019), 725-734.
10. Spyrakos, C., Koutromanos, I. and Maniatakis, C.A., "Seismic response of base-isolated buildings including soil–structure interaction", ***Soil Dynamics and Earthquake Engineering***, Vol. 29, No. 4, (2009), 658-668. https://doi.org/10.1016/j.soildyn.2008.07.002
11. Aydin, E., Ozturk, B., Bogdanovic, A. and Farsangi, E.N., "Influence of soil-structure interaction (ssi) on optimal design of passive damping devices", in Structures, Elsevier. Vol. 28, (2020), 847-862.
12. El-Bayoumi, K., Naguib, M. and Salem, F.A., "Dynamic analysis of high rise seismically isolated buildings", ***American Journal of Civil Engineering***, Vol. 3, No. 2, (2015), 43-50. doi: 10.11648/j.ajce.20150302.13
13. Flora, A., Perrone, G. and Cardone, D., "Evaluating collapse fragility curves for existing buildings retrofitted using seismic isolation", ***Applied Sciences***, Vol. 10, No. 8, (2020), 2844. https://doi.org/10.3390/app10082844
14. Castaldo, P., Palazzo, B. and Della Vecchia, P., "Seismic reliability of base-isolated structures with friction pendulum bearings", ***Engineering Structures***, Vol. 95, (2015), 80-93. https://doi.org/10.1016/j.soildyn.2019.105930
15. Peng, Y., Ma, Y., Huang, T. and De Domenico, D., "Reliability-based design optimization of adaptive sliding base isolation system for improving seismic performance of structures", ***Reliability Engineering & System Safety***, Vol. 205, (2021), 107167. https://doi.org/10.1016/j.ress.2020.107167
16. Barrera-Vargas, C.A., Díaz, I.M., Soria, J.M. and García-Palacios, J.H., "Enhancing friction pendulum isolation systems using passive and semi-active dampers", ***Applied Sciences***, Vol. 10, No. 16, (2020), 5621. https://doi.org/10.3390/app10165621
17. Hessabi, R.M., Mercan, O. and Ozturk, B., "Exploring the effects of tuned mass dampers on the seismic performance of structures with nonlinear base isolation systems", ***Earthquakes and Structures***, Vol. 12, No. 3, (2017), 285-296. http://dx.doi.org/10.12989/eas.2017.12.3.285
18. Ozturk, B., Cetin, H., Dutkiewicz, M., Aydin, E. and Noroozinejad Farsangi, E., "On the efficacy of a novel optimized tuned mass damper for minimizing dynamic responses of cantilever beams", ***Applied Sciences***, Vol. 12, No. 15, (2022), 7878. http://dx.doi.org/10.3390/app12157878
19. Sreeman, D. and Kumar Roy, B., "Optimization study of isolated building using shape memory alloy with friction pendulum system under near-fault excitations", ***International Journal of Engineering, Transactions B: Applications*** Vol. 35, No. 11, (2022), 2176-2185. http://dx.doi.org/10.5829/IJE.2022.35.11B.12
20. Yurdakul, M. and Yıldız, M.B., "A study on seismic isolation of building used lrb", ***Challenge***, Vol. 6, No. 2, (2020), 52-60. http://dx.doi.org/10.20528/cjsmec.2020.02.001
21. Rakicevic, Z., Bogdanovic, A., Farsangi, E.N. and Sivandi-Pour, A., "A hybrid seismic isolation system toward more resilient structures: Shaking table experiment and fragility analysis", ***Journal of Building Engineering***, Vol. 38, (2021), 102194. http://dx.doi.org/10.1016/j.jobe.2021.102194

22. Noroozinejad Farsangi, E., Tasnimi, A.A., Yang, T., Takewaki, I. and Mohammadhasani, M., "Seismic performance of base-isolated buildings under multi-directional earthquake excitations", ***Smart Struct. Syst***, Vol. 22, No. 4, (2018), 383-397. https://cir.nii.ac.jp/crid/1050282677492590720
23. Hayden, C.P., Bray, J.D. and Abrahamson, N.A., "Selection of near-fault pulse motions", ***Journal of Geotechnical and Geoenvironmental Engineering***, Vol. 140, No. 7, (2014), 04014030. http://dx.doi.org/10.1061/(ASCE)GT.1943-5606.0001129
24. Mavronicola, E.A., Polycarpou, P.C. and Komodromos, P., "Effect of ground motion directionality on the seismic response of base isolated buildings pounding against adjacent structures", ***Engineering Structures***, Vol. 207, (2020), 110202. https://doi.org/10.1016/j.engstruct.2020.110202
25. Jamalzadeh, A. and Barghian, M., "Dynamic response of a pendulum isolator system under vertical and horizontal earthquake excitation", ***Periodica Polytechnica Civil Engineering***, Vol. 59, No. 3, (2015), 433-440. https://doi.org/10.3311/PPci.7848
26. Cancellara, D. and De Angelis, F., "A base isolation system for structures subject to extreme seismic events characterized by anomalous values of intensity and frequency content", ***Composite Structures***, Vol. 157, (2016), 285-302. https://doi.org/10.1016/j.compstruct.2016.09.002
27. Providakis, C., "Effect of supplemental damping on lrb and fps seismic isolators under near-fault ground motions", ***Soil Dynamics and Earthquake Engineering***, Vol. 29, No. 1, (2009), 80-90. https://doi.org/10.1016/j.soildyn.2008.01.012
28. Rong, Q., "Optimum parameters of a five-story building supported by lead-rubber bearings under near-fault ground motions", ***Journal of Low Frequency Noise, Vibration and Active Control***, Vol. 39, No. 1, (2020), 98-113. http://dx.doi.org/10.1177/1461348419845829
29. Anajafi, H., Poursadr, K., Roohi, M. and Santini-Bell, E., "Effectiveness of seismic isolation for long-period structures subject to far-field and near-field excitations", ***Frontiers in Built Environment***, Vol. 6, (2020), 24. https://doi.org/10.3389/fbuil.2020.00024
30. Kilar, V. and Koren, D., "Seismic behaviour of asymmetric base isolated structures with various distributions of isolators", ***Engineering Structures***, Vol. 31, No. 4, (2009), 910-921. https://doi.org/10.1016/j.engstruct.2008.12.006
31. Choudhury, S.S. and Patro, S.K., Seismic control of soft storey buildings using lrb isolation system, in Recent developments in sustainable infrastructure: Select proceedings of icrdsi 2019. 2020, Springer.301-309.
32. Tena-Colunga, A. and Zambrana-Rojas, C., "Dynamic torsional amplifications of base-isolated structures with an eccentric isolation system", ***Engineering Structures***, Vol. 28, No. 1, (2006), 72-83. https://doi.org/10.1016/j.engstruct.2005.07.003
33. Özuygur, A.R. and Noroozinejad Farsangi, E., "Influence of pulse-like near-fault ground motions on the base-isolated buildings with lrb devices", ***Practice Periodical on Structural Design and Construction***, Vol. 26, No. 4, (2021), 04021027. http://dx.doi.org/10.1061/(ASCE)SC.1943-5576.0000603
34. Kaveh, A., "Advances in metaheuristic algorithms for optimal design of structures, Springer, (2014).
35. Danesh, M., "Evaluation of seismic performance of pbd optimized steel moment frames by means of neural network", ***Jordan Journal of Civil Engineering***, Vol. 13, No. 3, (2019). doi. https://jjce.just.edu.jo/issues/paper.php?p=4774.pdf
36. Dorigo, M. and Di Caro, G., "Ant colony optimization: A new meta-heuristic", in Proceedings of the 1999 congress on evolutionary computation-CEC99 (Cat. No. 99TH8406), IEEE. Vol. 2, (1999), 1470-1477.
37. Saremi, S., Mirjalili, S. and Lewis, A., "Grasshopper optimisation algorithm: Theory and application", ***Advances in Engineering Software***, Vol. 105, (2017), 30-47. https://doi.org/10.1016/j.advengsoft.2017.01.004
38. Abdeddaim, M., Djerouni, S., Ounis, A., Athamnia, B. and Farsangi, E.N., "Optimal design of magnetorheological damper for seismic response reduction of base-isolated structures considering soil-structure interaction", in Structures, Elsevier. Vol. 38, (2022), 733-752.
39. Naeim, F. and Kelly, J.M., "Design of seismic isolated structures: From theory to practice, John Wiley & Sons, (1999).
40. Code, I.H.G.D., "Vice presidency for strategic planning and supervision", ***Tehran, Iran: Ministry of Roads and Urban Development***, (2012). https://www.bhrc.ac.ir/Portals/8/PropertyAgent/1567/Files/1894/Code523.pdf
41. Newmark, N.M., "A method of computation for structural dynamics", ***Journal of the Engineering Mechanics Division***, Vol. 85, No. 3, (1959), 67-94. https://doi.org/10.1061/JMCEA3.0000098
42. Stanikzai, M.H., Elias, S., Matsagar, V.A. and Jain, A.K., "Seismic response control of base-isolated buildings using tuned mass damper", ***Australian Journal of Structural Engineering***, Vol. 21, No. 1, (2020), 310-321. https://doi.org/10.3390/app10041230
43. Ariga, T., Kanno, Y. and Takewaki, I., "Resonant behaviour of base-isolated high-rise buildings under long-period ground motions", ***The Structural Design of Tall and Special Buildings***, Vol. 15, No. 3, (2006), 325-338. http://dx.doi.org/10.1002/tal.298
44. Furukawa, T., Ito, M., Izawa, K. and Noori, M.N., "System identification of base-isolated building using seismic response data", ***Journal of Engineering Mechanics***, Vol. 131, No. 3, (2005), 268-275. http://dx.doi.org/10.1061/(ASCE)0733-9399(2005)131:3(268)

Persian Abstract

چکیده

پارامترهای مکانیکی و هندسی مختلف می‌توانند بر روی رفتار سیستم جداسازی پایه اثر داشته باشند. بنابراین، انجام تحلیل حساسیت رفتار سازه‌ی جداسازی شده یک امر ضروری است. در نتیجه، سیستم‌های جداسازی باید با روش‌های بهینه‌سازی طراحی شوند تا اثرات عوامل مختلف در آنها لحاظ گردد. در این مطالعه، کاربرد یک الگوریتم بهینه‌سازی جدید در طراحی سیستم‌های جداساز لاستیکی با هسته‌ی سربی (LRB) برای مقاوم‌سازی لرزه‌ای سازه‌های ساختمانی بررسی شد. تحلیل حساسیت رفتار ساختمان جداسازی شده با درنظر گرفتن خصوصیات مکانیکی سیستم جداساز و نامنظمی جرمی انجام گردید. در اینجا، تحلیل تاریخچه- زمان غیرخطی جهت تعیین پاسخ‌ها به کار رفت و همچنین طراحی بهینه‌ی جداساز در برنامه‌ی MATLAB با استفاده از الگوریتم جدید بهینه‌سازی ملخ (GOA) تهیه شد. اهداف اصلی بررسی قابلیت الگوریتم بهینه‌سازی ملخ در طراحی بهینه‌ی پارامترهای قاب‌های جداسازی شده با سیستم LRB بود. نتایج نشان دهنده‌ی قابلیت مطلوب این الگوریتم در طراحی این نوع سیستم جداساز بود. همچنین، تحلیل حساسیت پاسخ سازه‌ی جداسازی شده نشان داد که شاخص برش پایه‌ی تسلیم دارای بیشترین اثر روی پاسخ‌ها بود. نامنظمی جرمی نیز اثر ناچیزی در تحلیل حساسیت نشان داد.